

# Changes in productivity and redox conditions in the Panthalassic Ocean during the latest Permian

Thomas J. Algeo<sup>1</sup>, Linda Hinnov<sup>2</sup>, Jessa Moser<sup>1</sup>, J. Barry Maynard<sup>1</sup>, Erika Elswick<sup>3</sup>, Kiyoko Kuwahara<sup>4</sup>, and Hiroyoshi Sano<sup>5</sup>

<sup>1</sup>Department of Geology, University of Cincinnati, Cincinnati, Ohio 45221-0013, USA

<sup>2</sup>Department of Earth and Planetary Sciences, Johns Hopkins University, Baltimore, Maryland 21218, USA

<sup>3</sup>Department of Geological Sciences, Indiana University, Bloomington, Indiana 47405-1405, USA

<sup>4</sup>Department of Geology, Ashiya University, Ashiya 659-8511, Japan

<sup>5</sup>Department of Earth and Planetary Sciences, Kyushu University, Fukuoka 812-8581, Japan

## ABSTRACT

The Gujo-Hachiman section in central Japan provides a rare window into environmental conditions within the Panthalassic Ocean, which encompassed more than half the Earth's surface at 251 Ma. The section is characterized by a sharp transition from green-gray organic-poor cherts to black siliceous shales in the uppermost Permian. Normalization to the clay fraction demonstrates that apparent increases in the concentrations of organic matter and trace metals above this transition were due primarily to the loss of a diluent biogenic (radiolarian) silica flux and only secondarily to a small shift toward more reducing bottom waters. In the black shale, pyrite abundance increases by a factor of ~30× and is dominated by framboidal grains of probable syngenetic origin. These observations suggest that the expansion of low-oxygen conditions within the Panthalassic Ocean was focused within the oxygen-minimum zone rather than at the seafloor. Such a pattern implies that (1) changes in nutrient fluxes and primary productivity rates, rather than stagnation of oceanic circulation, were a key factor influencing oceanic redox conditions around the Permian-Triassic boundary, and (2) large regions of the Panthalassic Ocean underwent only limited redox changes, providing potential refugia for marine taxa that survived into the Triassic.

## INTRODUCTION

The ca. 251 Ma Permian-Triassic (P-Tr) boundary mass extinction was the largest biotic catastrophe of the Phanerozoic Eon, resulting in the disappearance of ~90% of marine and terrestrial species (Erwin, 2006). Many contemporaneous shallow-marine platforms developed euxinic conditions, i.e., a lack of dissolved oxygen along with free H<sub>2</sub>S in the water column (Nielsen and Shen, 2004; Grice et al., 2005; Wignall et al., 2005; Riccardi et al., 2006; Cao et al., 2009). Most such records are from the Tethyan region, which composed only 10%–15% of the global ocean and formed an equatorial cul de sac that may have acted as a nutrient trap, resulting in high levels of productivity and oxygen demand (Winguth and Maier-Reimer, 2005). Redox conditions in the larger Panthalassic Ocean, comprising 85%–90% of the contemporaneous global ocean, are less well known owing to later subduction of most Permian–Triassic oceanic crust. The only surviving Panthalassic seafloor sediments are within accretionary terranes now located in Japan, New Zealand, and western Canada (Isozaki, 1997a). In this study we examined the petrography and geochemistry of a P-Tr boundary deep-sea succession in Japan in order to gain new insights concerning redox and other environmental conditions within Panthalassa.

## GEOLOGIC SETTING

The Gujo-Hachiman section near Itadori, Japan, is within the Mino-Tanba Belt, a sub-

duction-generated accretionary complex consisting chiefly of Middle and Late Jurassic terrigenous clastics containing exotic blocks of Permian–Middle Jurassic oceanic assemblages (Fig. 1A; Isozaki, 1997a). During the Triassic, the study site was located in the equatorial Panthalassic Ocean (Ando et al., 2001). The section consists of a lower 7.0-m-thick chert unit and an upper 65-cm-thick black shale unit. Radiolarian biostratigraphy supports a middle to late Changxingian age for the chert unit as well as for the basal 40 cm of the black shale unit, which contains a few thin fossil-bearing siliceous laminae (Kuwahara and Yao, 2001; Yao et al., 2001). The remainder of the black

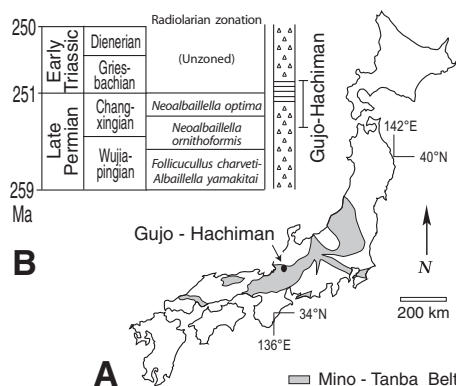


Figure 1. Gujo-Hachiman section, central Japan. A: Location map. B: Stratigraphy (modified from Kuwahara and Yao, 2001).

shale unit is barren of fossils, rendering exact placement of the P-Tr boundary uncertain (for biostratigraphic age control, see the GSA Data Repository<sup>1</sup>). Younger chert beds (not studied here) overlying the black shale yielded conodonts of Dienerian–Spathian age (Yamakitai, 1987). Sedimentation rates for the Upper Permian chert unit averaged ~7–8 m m.y.<sup>-1</sup> (based on spectral analysis; see following), consistent with slow accumulation in an abyssal setting.

## RESULTS

Chert abundance decreases from 89% ± 5% in the chert unit to 51% ± 8% in the black shale, while illite concurrently increases from 9% ± 5% to 44 ± 8%, with other components composing <5% of most samples (Fig. 2A). Accompanying the lithologic transition are sharp rises in the concentrations of Al (from 1.1% ± 0.6% to 5.2% ± 0.9%), TOC (from 0.2% ± 0.1% to 1.2 ± 0.5%), and S (from 0.1% ± 0.1% to 1.6% ± 0.6%; Figs. 2C–2E). Many elements show increases of similar magnitude, with Al and most detrital elements enriched by factors of 4–5× and total organic carbon (TOC) and redox-sensitive metals (Mo, U, V) enriched by factors of 6–8× (Table 1). The only major elements to fall outside this range of enrichment factors are S (30×) and Fe (1.9×).

The character of the pyrite fraction changes abruptly at the lithologic contact. Pyrite abundance (by point count) increases from 1%–2% in the chert unit to 10%–22% in the black shale (Fig. 3A). In the former, pyrite grains are entirely euhedral and mostly of small size (<2 μm; Fig. 3B). In the latter, ~50%–90% of pyrite grains are framboids with diameters of 5–10 μm, and the lesser fraction of euhedral grains tends toward much larger sizes (to 250 μm). Average δ<sup>34</sup>S<sub>py</sub> values shift from -26.8‰ ± 3.1‰ in the chert unit (n = 16) to -33.3‰ ± 3.6‰ in the black shale (n = 9; data not shown), similar to P-Tr boundary S isotopic shifts reported in other studies (Kajiwa-

<sup>1</sup>GSA Data Repository item 2010037, biostratigraphic age control, and methods, is available online at [www.geosociety.org/pubs/ft2010.htm](http://www.geosociety.org/pubs/ft2010.htm), or on request from [editing@geosociety.org](mailto:editing@geosociety.org) or Documents Secretary, GSA, P.O. Box 9140, Boulder, CO 80301, USA.

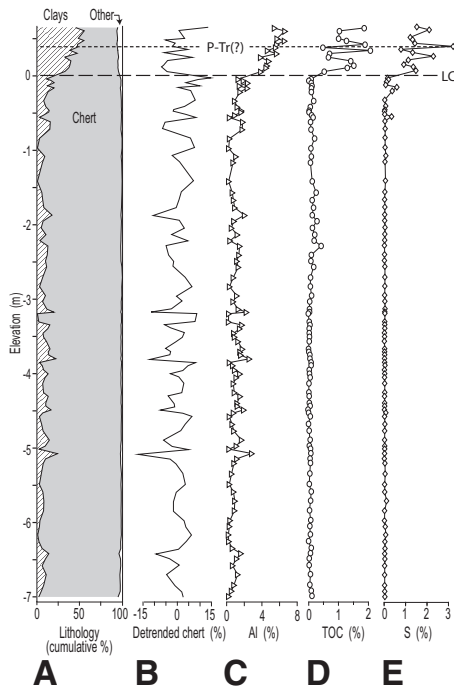


**Figure 2. A: Lithology. B: Detrended chert abundance (25% weighted-average LOWESS (locally weighted scatterplot smoothing) curve subtracted from percent chert in panel A). C: Aluminum. D: Total organic carbon (TOC). E: Total sulfur. Elevations relative to lithologic contact (LC) between chert and black shale units; position of Permian-Triassic (P/Tr) boundary is approximate.**

TABLE 1. GUJO-HACHIMAN ELEMENTAL DATA

	Ch avg*	BS avg*	X <sub>BS/Ch</sub> <sup>†</sup>	(X/Al) <sub>BS/Ch</sub> <sup>†</sup>
S (ppm)	51	1548	30.43	6.32
Mo (ppm)	2.7	21.5	8.06	1.67
U (ppm)	1.1	8.1	7.72	1.60
V (ppm)	37	272	7.25	1.50
TOC (%)	0.2	1.2	6.45	1.34
Al (%)	1.1	5.2	4.82	1.00
P (ppm)	118	555	4.71	0.97
Co (ppm)	4.0	17.7	4.49	0.94
K (%)	0.5	2.2	4.30	0.90
Mg (%)	0.2	1.0	4.26	0.89
Zn (ppm)	30	122	4.05	0.85
Ni (ppm)	20	78	3.93	0.82
Ti (ppm)	718	2801	3.90	0.81
Fe (%)	1.5	2.8	1.86	0.39
SiO <sub>2</sub> -bulk (%)	92.4	74.0	0.80	0.17
SiO <sub>2</sub> -biogenic (%)	89.4	51.1	0.57	0.12

Note: TOC—total organic carbon.

\*Average elemental concentrations for the chert (Ch) and black shale (BS) units.

<sup>†</sup>Concentration ratios on a raw (X) and Al-normalized (X/Al) basis.

et al., 1994; Nielsen and Shen, 2004; Algeo et al., 2008). Total S exhibits negative covariation with TOC [ $r = -0.62$ ,  $n = 13$ ,  $p(\alpha) < 0.05$ ] for samples containing  $>0.5\%$  TOC, consistent with Fe limitation of pyrite formation (Raiswell and Berner, 1985).

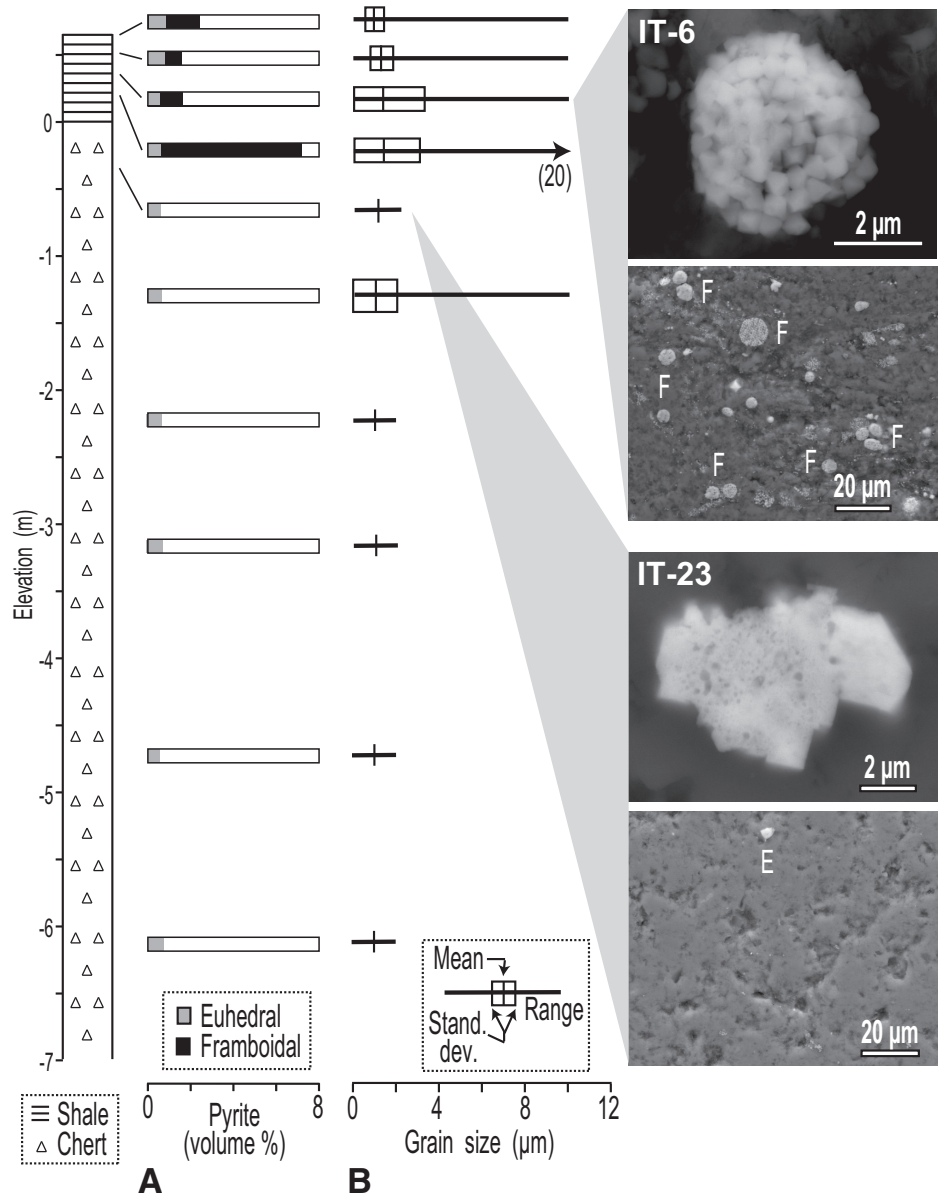


**Figure 3. A: Volumetric abundance of pyrite by grain type. B: Grain size. C: Scanning electron microscope photos of representative samples for chert (IT-23) and black shale units (IT-6). E—euhedral, F—framboidal.**

The study section exhibits pronounced lithologic cyclicity at a submeter scale (Fig. 2A). To investigate its significance, we analyzed the detrended chert record (Fig. 2B) using spectral techniques. The whole-section power spectrum exhibits a dominant peak at  $\sim 65$  cm and secondary peaks at 144, 40, 27, and 21 cm (Fig. 4A). If the 65 cm peak represents forcing by the 100 k.y. short eccentricity cycle (note that other orbital periodicities yield durations for the section that are inconsistent with existing geochronologic constraints), then the 7.0-m-thick chert unit accumulated in  $\sim 1.1$  m.y. The evolutionary power spectrum (Fig. 4B) confirms the positions and persistence of the spectral peaks and shows that (1) the 65 cm peak undergoes repeated bifurca-

tions upsection, possibly related to frequency modulations expected for the 100 k.y. short eccentricity cycle; (2) frequencies  $>0.02$  cycles/cm are evident mainly within a high-resolution sampling interval in the middle of the study section; and (3) a pronounced shift toward higher frequencies occurs near the top of the section, implying a large decrease in bulk accumulation rates. Thinning of cycles from 65 cm in the chert unit to  $\sim 16$  cm in the black shale (see Fig. 2B) suggests an  $\sim 4\times$  decrease in bulk accumulation rates, a pattern supported by sinking flux changes.

### SINKING FLUX CHANGES

Most changes in the bulk chemistry of the study section can be accounted for through

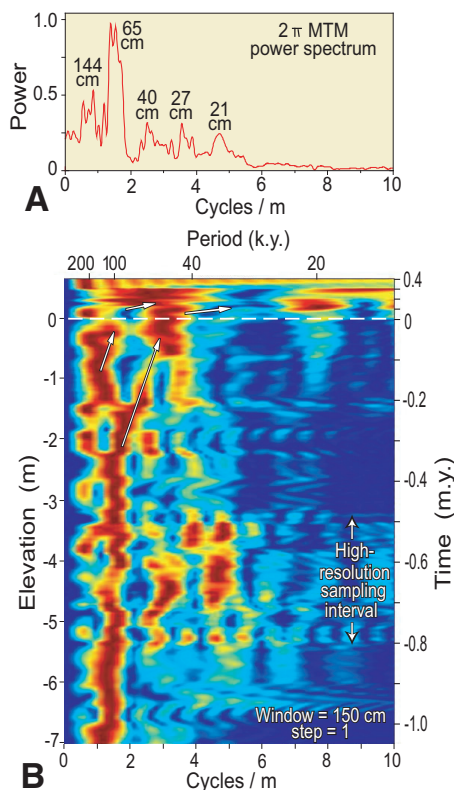


**Figure 4. Spectral analysis. A:**  $2\pi$  multitaper method (MTM) spectrum of entire section. **B:** Evolutionary spectrogram using 150 cm window; magnitude-squared Fourier transforms are displayed. Chert data (Fig. 2B) were interpolated from uneven sample spacing ( $7.7 \pm 3.8$  cm) to even spacing of 1 cm. Higher frequencies at  $-3.3$  to  $-5.3$  m may represent obliquity and precession signals that are marginally resolved within this interval of more closely spaced samples. Note general shift toward higher frequencies toward top of section (arrows). Vertical axis at right is scaled relative to lithologic contact and reflects  $\sim 4\times$  decrease in bulk accumulation rates within black shale. Res.—resolution.

secular variation in the sinking flux of biogenic (radiolarian) silica. The decrease in chert across the lithologic contact corresponds to a  $4.6\times$  reduction in the sinking flux of biogenic silica, which is the inverse of the  $4\text{--}5\times$  enrichments observed for detrital elements such as Al, K, and Ti (Table 1). The slightly greater ( $6\text{--}8\times$ ) enrichment of TOC and redox-sensitive metals (Mo, U, V) can be interpreted as due primarily ( $60\%\text{--}80\%$ ) to a reduced biogenic silica flux and secondarily ( $20\%\text{--}40\%$ ) to other factors (e.g., enhanced sinking flux of organic matter, more reducing conditions). However, increases in S are large for both raw ( $30\times$ ) and Al-normalized concentrations ( $6.3\times$ ), indicating a substantial increase in the sinking flux of S linked to the appearance of pyrite framboids during black shale deposition. The  $61\%$  decrease in the Al-normalized concentration of Fe (Table 1)

may reflect stronger scavenging of Fe in more proximal regions of the global ocean as euxinia spread during the latest Permian.

### REDOX CONDITIONS

The transition from light-colored cherts to black shales in the uppermost Permian of Japanese deep-ocean sections has been cited as evidence of a shift from oxic to euxinic conditions within the Panthalassic Ocean and, hence, of a redox event of global or near-global extent (Wignall and Twitchett, 1996; Isozaki, 1997b). However, evidence presented here shows that most changes in the Gujo-Hachiman section are attributable to a sustained  $4\text{--}5\times$  reduction in the sinking flux of biogenic silica in the latest Permian. After accounting for variation in this flux, only limited increases in TOC ( $1.3\times$ ) and redox-sensitive metals ( $1.5\text{--}1.7\times$ ) are observed across the chert-black shale contact (Table 1), suggesting that Panthalassic deep waters were only slightly more oxygen deficient at the peak of the P-Tr boundary crisis than they were previously. This inference is consistent with biofabric evidence from other Japanese P-Tr boundary sections indicative of a shift from oxic to suboxic conditions (Kakuwa, 2008) rather than to euxinic conditions.

Changes in the pyrite fraction nonetheless provide evidence of euxinia during deposition of the black shale unit. Pyrite framboids are spherical aggregates of submicron-sized crystals with a raspberry-like appearance that form via the reaction of  $\text{H}_2\text{S}$  with iron particles through monosulfide intermediates (Wilkin et al., 1996). Syngenetic framboids (i.e., those formed in a  $\text{H}_2\text{S}$ -bearing water column) generally do not exceed  $\sim 5\text{--}7$   $\mu\text{m}$  in diameter as a consequence of the rapid settling of larger particles from suspension. Framboidal pyrite usually yields more  $^{34}\text{S}$ -depleted compositions than diagenetic pyrite owing to near-maximum fractionation during bacterial sulfate reduction within a sulfate-unlimited reservoir such as the open ocean (Wilkin and Arthur, 2001). The abundant small  $^{34}\text{S}$ -depleted framboids in the black shale unit at Gujo-Hachiman (Fig. 3) probably formed in a euxinic water mass. This observation can be reconciled with an inference of suboxic bottom waters if the framboids formed higher in the water column, e.g., within the oxygen-minimum zone (OMZ) at  $\sim 500\text{--}1000$  m water depth (and thus several kilometers above the Panthalassic seafloor). The slightly larger modal diameter of these framboids ( $5\text{--}10$   $\mu\text{m}$ ) relative to those in modern euxinic settings ( $4\text{--}5$   $\mu\text{m}$ ; Wilkin et al., 1996) may be a consequence of a longer settling time or a larger mean size of settling fecal pellets.

### OCEANIC PRODUCTIVITY

Changes in marine primary productivity may have played an important role in the P-Tr

boundary crisis. Elevated TOC values in P-Tr boundary black shales in Japan have been cited as evidence for elevated levels of primary productivity that may have contributed to deep-water anoxia in the Panthalassic Ocean (Suzuki et al., 1998). Other studies have noted rapid fluctuations in radiolarian abundance during the latest Permian followed by a population crash at the P-Tr boundary, possibly due to reduced nutrient availability linked to environmental disturbances or climate change (Beauchamp and Baud, 2002; Isozaki et al., 2007). The decimation of radiolarians during the boundary crisis, reflected in a  $4\text{--}5\times$  decrease in the flux of biogenic silica at Gujo-Hachiman, implies major changes at the base of the marine food chain, such as a substantial reduction in productivity or a shift toward primary producers not favored by radiolarians (e.g., green sulfur bacteria; Grice et al., 2005; Cao et al., 2009). Radiolarians did not begin to recover in diversity or biomass until the late Olenekian Stage,  $\sim 3\text{--}4$  m.y. after the P-Tr boundary crisis (Kozur, 1998).

### GENERAL IMPLICATIONS

The underlying causes of marine environmental deterioration during the Permian–Triassic remain under discussion. Sustained stagnation of global ocean circulation has been inferred (Kajiwara et al., 1994; Wignall and Twitchett, 1996; Isozaki, 1997b), but challenged as unlikely on the basis of paleoceanographic modeling (Hotinski et al., 2001). Reduced dissolved oxygen levels in Permian–Triassic seawater have been linked instead to changes in sea-surface temperatures, freshwater fluxes, nutrient levels, and particle penetration depths, and model results suggest that low-oxygen conditions expanded most dramatically within the OMZ rather than at abyssal depths (Hotinski et al., 2001; Kiehl and Shields, 2005; Winguth and Maier-Reimer, 2005). The results of the present study are consistent with these results and contribute to a resolution of apparent model-data discrepancies. An expanded, sulfidic OMZ provided a source for toxic  $\text{H}_2\text{S}$ -bearing waters that episodically upwelled onto shallow continental shelves and platforms around the P-Tr boundary (Algeo et al., 2008). Because intensification of the OMZ is also projected to be a consequence of modern climatic warming (Shaffer et al., 2009), oceanographic conditions during the P-Tr boundary crisis have present-day relevance.

The hypothesis of only limited changes in dissolved oxygen levels in Panthalassa also has implications for the post-crisis recovery process. The reappearance of many warm-water forms at the end of the Early Triassic suggests that these organisms must have occupied refugia for  $\sim 3\text{--}4$  m.y. following the P-Tr boundary crisis (Kozur, 1998). Many of these Lazarus

taxa had lifestyles conducive to survival under low-oxygen conditions (Bottjer et al., 2008). If redox conditions in the Panthalassic Ocean were less intensely reducing than in the Tethys Ocean, the former may have provided the necessary refugia. Finally, recognition of orbital periodicities in the study section may assist in development of a “floating” astronomical time scale across the P-Tr boundary and provide a basis for ultrahigh-resolution global correlations (Hinnov, 2000).

#### ACKNOWLEDGMENTS

We thank Yukio Isozaki and two anonymous reviewers for their comments. This research was supported by National Science Foundation grants EAR-0618003 and EAR-0745574 to Algeo.

#### REFERENCES CITED

- Algeo, T.J., Shen, Y., Zhang, T., Lyons, T., Bates, S., Rowe, H., and Nguyen, T.K.T., 2008, Association of  $^{34}\text{S}$ -depleted pyrite layers with negative carbonate  $\delta^{13}\text{C}$  excursions at the Permian-Triassic boundary: Evidence for upwelling of sulfidic deep-ocean water masses: *Geochemistry Geophysics Geosystems*, v. 9, Q04025, doi: 10.1029/2007GC001823.
- Ando, A., Kodama, K., and Kojima, S., 2001, Low-latitude and Southern Hemisphere origin of Anisian (Triassic) bedded chert in the Inuyama area, Mino terrane, central Japan: *Journal of Geophysical Research*, v. 106, no. B2, p. 1973–1986, doi: 10.1029/2000JB900305.
- Beauchamp, B., and Baud, A., 2002, Growth and demise of Permian biogenic chert along northwest Pangea: Evidence for end-Permian collapse of thermohaline circulation: *Palaeogeography, Palaeoclimatology, Palaeoecology*, v. 184, p. 37–63, doi: 10.1016/S0031-0182(02)00245-6.
- Bottjer, D.J., Clapham, M.E., Fraiser, M.L., and Powers, C.M., 2008, Understanding mechanisms for the end-Permian mass extinction and the protracted Early Triassic aftermath and recovery: *GSA Today*, v. 18, no. 9, p. 4–10, doi: 10.1130/GSATG8A.1.
- Cao, C., Love, G.D., Hays, L.E., Wang, W., Shen, S., and Summons, R.E., 2009, Biogeochemical evidence for euxinic oceans and ecological disturbance presaging the end-Permian mass extinction event: *Earth and Planetary Science Letters*, v. 281, p. 188–201, doi: 10.1016/j.epsl.2009.02.012.
- Erwin, D.L., 2006, *Extinction. How life on Earth nearly ended 250 million years ago*: Princeton, New Jersey, Princeton University Press, 296 p.
- Grice, K., Cao, C., Love, G.D., Böttcher, M.E., Twitchett, R.J., Grosjean, E., Summons, R.E., Turgeon, S.C., Dunning, W., and Jin, Y., 2005, Photic zone euxinia during the Permian-Triassic superanoxic event: *Science*, v. 307, p. 706–709, doi: 10.1126/science.1104323.
- Hinnov, L.A., 2000, New perspectives on orbitally forced stratigraphy: *Annual Review of Earth and Planetary Sciences*, v. 28, p. 419–475, doi: 10.1146/annurev.earth.28.1.419.
- Hotinski, R.M., Bice, K.L., Kump, L.R., Najjar, R.G., and Arthur, M.A., 2001, Ocean stagnation and end-Permian anoxia: *Geology*, v. 29, p. 7–10, doi: 10.1130/0091-7613(2001)029<0007:OSAEP A>2.0.CO;2.
- Isozaki, Y., 1997a, Jurassic accretion tectonics of Japan: *The Island Arc*, v. 6, p. 25–52, doi: 10.1111/j.1440-1738.1997.tb00039.x.
- Isozaki, Y., 1997b, Permo-Triassic boundary superanoxia and stratified superocean; records from lost deep sea: *Science*, v. 276, p. 235–238, doi: 10.1126/science.276.5310.235.
- Isozaki, Y., Shimizu, N., Yao, J., Ji, Z., and Matsuda, T., 2007, End-Permian extinction and volcanism-induced environmental stress: Permian-Triassic boundary interval of a lower-slope facies at Chaotian, South China: *Palaeogeography, Palaeoclimatology, Palaeoecology*, v. 252, p. 218–238, doi: 10.1016/j.palaeo.2006.11.051.
- Kajiwar, Y., Yamakita, S., Ishida, K., Ishiga, H., and Imai, A., 1994, Development of a largely anoxic stratified ocean and its temporary massive mixing at the Permian/Triassic boundary supported by the sulfur isotope record: *Palaeogeography, Palaeoclimatology, Palaeoecology*, v. 111, p. 367–379, doi: 10.1016/0031-0182(94)90072-8.
- Kakuwa, Y., 2008, Evaluation of palaeo-oxygenation of the ocean bottom across the Permian-Triassic boundary: *Global and Planetary Change*, v. 63, p. 40–56, doi: 10.1016/j.gloplacha.2008.05.002.
- Kiehl, J.T., and Shields, C.A., 2005, Climate simulation of the latest Permian: Implications for mass extinction: *Geology*, v. 33, p. 757–760, doi: 10.1130/G21654.1.
- Kozur, H.W., 1998, Some aspects of the Permian-Triassic boundary (PTB) and of the possible causes for the biotic crisis around this boundary: *Palaeogeography, Palaeoclimatology, Palaeoecology*, v. 143, p. 227–272, doi: 10.1016/S0031-0182(98)00113-8.
- Kuwahara, K., and Yao, A., 2001, Late Permian radiolarian faunal change in bedded chert of the Mino Belt, Japan: *News of Osaka Micropaleontologists*, v. 12, p. 33–49.
- Nielsen, J.K., and Shen, Y., 2004, Evidence for sulfidic deep water during the Late Permian in the East Greenland Basin: *Geology*, v. 32, p. 1037–1040, doi: 10.1130/G20987.1.
- Raiswell, R., and Berner, R.A., 1985, Pyrite formation in euxinic and semi-euxinic sediments: *American Journal of Science*, v. 285, p. 710–724.
- Riccardi, A., Arthur, M.A., and Kump, L.R., 2006, Sulfur isotopic evidence for chemocline upward excursions during the end-Permian mass extinction: *Geochimica et Cosmochimica Acta*, v. 70, p. 5740–5752, doi: 10.1016/j.gca.2006.08.005.
- Shaffer, G., Olsen, S.M., and Pedersen, J.O.P., 2009, Long-term ocean oxygen depletion in response to carbon dioxide emissions from fossil fuels: *Nature Geoscience*, v. 2, p. 105–109, doi: 10.1038/ngeo420.
- Suzuki, N., Ishida, K., Shinomiya, Y., and Ishiga, H., 1998, High productivity in the earliest Triassic ocean: Black shales, southwest Japan: *Palaeogeography, Palaeoclimatology, Palaeoecology*, v. 141, p. 53–65, doi: 10.1016/S0031-0182(98)00009-1.
- Wignall, P.B., and Twitchett, R.J., 1996, Oceanic anoxia and the end Permian mass extinction: *Science*, v. 272, p. 1155–1158, doi: 10.1126/science.272.5265.1155.
- Wignall, P.B., Newton, R., and Brookfield, M.E., 2005, Pyrite framboid evidence for oxygen-poor deposition during the Permian-Triassic crisis in Kashmir: *Palaeogeography, Palaeoclimatology, Palaeoecology*, v. 216, p. 183–188, doi: 10.1016/j.palaeo.2004.10.009.
- Wilkin, R.T., and Arthur, M.A., 2001, Variations in pyrite texture, sulfur isotope composition, and iron systematics in the Black Sea; evidence for late Pleistocene to Holocene excursions of the  $\text{O}_2$ - $\text{H}_2\text{S}$  redox transition: *Geochimica et Cosmochimica Acta*, v. 65, p. 1399–1416, doi: 10.1016/S0016-7037(01)00552-X.
- Wilkin, R.T., Barnes, H.L., and Brantley, S.L., 1996, The size distribution of framboidal pyrite in modern sediments: An indicator of redox conditions: *Geochimica et Cosmochimica Acta*, v. 60, p. 3897–3912, doi: 10.1016/0016-7037(96)00209-8.
- Winguth, A.M.E., and Maier-Reimer, E., 2005, Causes of marine productivity and oxygen changes associated with the Permian-Triassic boundary: A reevaluation with ocean general circulation models: *Marine Geology*, v. 217, p. 283–304, doi: 10.1016/j.margeo.2005.02.011.
- Yamakita, S., 1987, Stratigraphic relationship between Permian and Triassic strata of chert facies in the Chichibu Terrane in eastern Shikoku: *Geological Society of Japan Journal*, v. 93, p. 145–148.
- Yao, J., Yao, A., and Kuwahara, K., 2001, Upper Permian biostratigraphic correlation between conodont and radiolarian zones in the Tamba-Mino Terrane, southwest Japan: *Journal of Geosciences, Osaka City University*, v. 44, p. 97–119.

Manuscript received 22 June 2009

Revised manuscript received 10 September 2009

Manuscript accepted 14 September 2009

Printed in USA